DP-MS-75-54

HYDROGEN TRANSPORT AND EMBRITTLEMENT IN STRUCTURAL METALS

by

M. R. Louthan, Jr.
and
G. R. Caskey, Jr.

Savannah River Laboratory
E. I. du Pont de Nemours & Co.
Aiken, South Carolina 29801

For presentation at the
1st World Hydrogen Energy Conference
to be held in Miami Beach, Florida
March 1-3, 1976, and for
publication in the proceedings.

This document was prepared in conjunction with work accomplished under Contract No. AT(07-2)-1 with the U.S. Department of Energy.

DISCLAIMER

HYDROGEN TRANSPORT AND EMBRITTLEMENT IN STRUCTURAL METALS*

M. R. Louthan, Jr. and G. R. Caskey, Jr.
Savannah River Laboratory
E. I. du Pont de Nemours & Co.
Aiken, South Carolina U.S.A.

ABSTRACT

The close relationship between hydrogen transport and embrittlement is indicated by available evidence of hydrogen absorption preceding degradation of mechanical properties. Furthermore, concentration of the hydrogen at a crack or flaw by diffusion or by transport with moving dislocations is probably necessary also. Permeation studies provide information on both absorption and diffusion of hydrogen. Experimental studies show that permeation of hydrogen is significantly influenced by surface conditions, particularly oxide films, and internal defects and impurities that trap diffusing hydrogen. The usual thermodynamic and diffusion relations, therefore, do not predict accurately the final distribution of hydrogen and the kinetics of the processes. Mathematical models that describe these effects are available; however, detailed interpretation of experimental data is not yet possible.

Investigation of the effects of hydrogen on the mechanical properties of approximately fifty structural alloys at ambient temperature and pressures up to 69 MPa indicates that all alloys show evidence of susceptibility to hydrogen embrittlement. Ferritic steels and nickel-base superalloys are strongly embrittled, austenitic steels are less affected, and aluminum alloys and copper alloys are relatively unaffected. The degree of hydrogen embrittlement appears to be related to the amount of hydrogen absorbed and its distribution within the metal lattice. Variables such as surface condition, defect structure, hydrogen purity, and hydrogen pressure have a significant influence on embrittlement. Of major importance is the transport of hydrogen with moving dislocations, a mechanism for concentration and redistribution of hydrogen that is operative at temperatures lower than for diffusion.

INTRODUCTION

Hydrogen compatibility is a basic material requirement for prospective structural and equipment components for a hydrogen energy-related economy. Potential deleterious effects of hydrogen environments on the integrity of storage tanks, reaction vessels, pipelines, and compressors are well documented: storage tanks fabricated from A517-F and 1146a steels have cracked under hydrogen pressures between 25 and 35 MPa [1], pipeline steels currently used for transport of natural gas are known to be susceptible to hydrogen-induced degradation of mechanical properties [2], and exposure to hydrogen environments increases the creep [3] and fatigue-crack growth [4] rates in several structural alloys. The list of susceptible materials continually increases with the demand for hydrogen-compatible alloys.

* The information contained in this article was developed during the course of work under Contract No. AT(07-2)-1 with the U.S. Energy Research and Development Administration.

Fusion power, hydride storage devices, high-pressure hydrogen systems, sour gas wells, and coal gasification plants all require structural alloys that resist hydrogen damage. Furthermore, alloys exposed to hydrogen often must have very low permeabilities to hydrogen to ensure containment, particularly in a tritium-containing fusion system. The Savannah River Laboratory (SRL) has been evaluating the compatibilities of commercial alloys with high-pressure hydrogen since about 1960; effects of hydrogen on the room-temperature tensile properties have been emphasized, and the temperature dependence of the permeability to hydrogen has been measured. Approximately fifty alloys have been studied, and many of the results have been published [5-25]. This paper includes a summary of published results, new data for several alloys, and an explanation of much of the data in terms of diffusion and interaction of hydrogen with microscopic defects in the alloys.

EXPERIMENTAL TECHNIQUES

The room-temperature ($\sim$295°K) tensile properties were generally determined on as-machined (32 rms finish) smooth bar specimens that were 5 cm long by 0.6 cm in diameter. Tests were made in room air and in hydrogen or helium at pressures to 69 MPa. Specimens were tested in both the as-received and hydrogen-charged conditions; the hydrogen-charged condition was used to simulate [24] long exposures to high-pressure gaseous hydrogen. Detailed experimental techniques have been previously described [9].

The permeability of an alloy to hydrogen was determined by measurements of the temperature-time dependence of the deuterium flux through both annealed and cold-worked foil specimens. Surface condition was found to have a significant influence on permeation rates, both during the permeation transient and at steady state. To minimize surface effects, foils were often tested while in contact with LiD powders. The LiD reduced the surface oxide films on many of the alloys thus allowing measurements of diffusion-controlled permeation. Additional experimental details are available in References 5 and 11.

Hydrogen Permeation

The flux of hydrogen (P) through a metallic wall depends in general on the permeability (ϕ) of the material in the wall, the area (A) and thickness (t) of the wall, and the driving force (F). For metals, where the molecular hydrogen gas dissociates at the gas-metal interface, dissolves, and then diffuses within the metal as an atom, the driving force is equal to the difference between the square root of the hydrogen pressures on the two sides of the wall, i.e., $F = \sqrt{p_1} - \sqrt{p_2}$. Formulae for calculating the rate of flow and total quantity of hydrogen that passes through plane, cylindrical, and spherical walls are available in standard references. To apply these formulae to specific cases, experimental data on permeability over the temperature and pressure range of interest is required.

Permeabilities of several pure metals and numerous commercial alloys were measured at Savannah River with deuterium gas at pressures of one to five atmospheres. The data are grouped as pure metals, ferrous alloys, and copper alloys, and are displayed in FIG. 1 to 3. The ferrous alloys include "MarzGrade"* iron, "Armco"** iron, T-1 steel, 4130 steel, "Kovar"†, HP-9-4-20, and several varieties of austenitic stainless steels. Oxygen-free and several types of deoxized copper were measured as well as three copper alloys, aluminum bronze, 70/30 brass, and "Berylco-25."†† All data are given in the International System (SI) of units where permeability is given in units of (mole/sec) $(m^2/m\sqrt{MPa})$ and temperature is in degrees Kelvin. To convert to metric, (cc/sec) $(cm^2/cm\sqrt{atm})$ units, multiply the permeability SI units by 71.38,

Generally, as shown in FIG. 2, the highest permeabilities are observed in the iron base alloys and the transition metals, nickel, cobalt, and platinum. Aluminum alloys and copper alloys have low permeabilities, due in part to the relatively low solubility of hydrogen in these materials. In addition, the adherent oxide films that form on aluminum alloys retard hydrogen permeation, as seen in FIG. 4. The presence of LiD in contact with the specimen surface increases the permeation, an effect believed to be associated with dehydration of the oxide [25]. The situation is different in the case of stainless steel, where the oxides are probably reduced by LiD. Thus the higher permeability (FIG. 5) when LiD is present is due to removal of the oxide [5].

Mechanical Properties

The room-temperature tensile properties of the alloys tested are summarized in TABLES I through XII. Copper alloys and aluminum alloys were not generally affected by hydrogen significantly. The lack of embrittlement in these two classes of alloys is in general agreement with other studies [26,27]. Fracture mechanics studies have confirmed the resistance of aluminum alloys to slow crack growth in dry gaseous hydrogen; however, both macroscopic and microscopic evidence have been reported for a mechanism of stress-corrosion cracking of aluminum alloys that depends on hydrogen embrittlement [28]. A mechanism that includes hydrogen embrittlement requires the generation of hydrogen at a high fugacity, probably by the reaction

$$Al + 3H_2O \rightarrow Al_2O_3 + 6H^+ + 6e^-$$

---

* Trademark of Materials Research Corp. for high purity iron.

** Trademark of Armco Steel Co. for pure iron.

† Trademark of Westinghouse Electric Co. for 29% Ni, 17% Co, 0.2% Mn, balance iron.

†† Trademark of Kawecki-Berylco Industries for 2% Be, 0.3% Co, balance copper.

and thus in many respects may be similar to hydrogen blistering [8]. Copper alloys may also be susceptible to hydrogen embrittlement at high hydrogen concentrations. High-purity copper charged with hydrogen by exposure at elevated temperatures showed hydrogen-induced reductions in both strength and ductility in subsequent tests at room temperature. Furthermore, earlier studies [29] have shown that the fracture mode of oxide-free high-conductivity copper is changed by exposure to 69-MPa hydrogen. Thus, as has been previously proposed [9], the lack of hydrogen embrittlement in both copper alloys and aluminum alloys is probably due to the low hydrogen solubility rather than intrinsic compatibility of the alloys with hydrogen.

Iron-, nickel-, and titanium-based alloys are all susceptible to hydrogen embrittlement. The extent of embrittlement depends on the specimen surface finish [7], the pretest exposure conditions, and hydrogen pressure during testing. In general, as-machined surfaces were more susceptible to hydrogen effects than were polished surfaces, and exposure conditions which enhanced hydrogen uptake increased the degree of embrittlement. Within a given family of alloys, the degree of embrittlement also correlated with dislocation substructure [9]; co-planar dislocation motion tends to promote embrittlement.

The effect of alloy strength on susceptibility to hydrogen embrittlement depended on the alloy system. The strength of austenitic steels, for example, apparently had little effect on susceptibility; as-machined Type 304L specimens with yield strengths as low as 200 MN/m^2 were severely embrittled, whereas HERF 304L with a 550 MN/m^2 yield was unaffected. However, the degree of embrittlement of nickel-based superalloys increased with increasing yield strength [FIG. 9 in REF. 9].

Although the results of the room temperature mechanical tests show that susceptibility to hydrogen embrittlement depends on many variables, all of the data are consistent with the hypothesis that hydrogen absorption must precede hydrogen-induced losses in mechanical properties. Clearly, absorption is minimized by surface treatments which inhibit hydrogen permeation. Furthermore, it is likely that many alloys show good hydrogen compatibility under specific exposure conditions where hydrogen absorption is reduced. For example, electropolishing has been shown [19] to increase the compatibility of Type 304L stainless steel with high-pressure hydrogen. Other studies [5] have shown that electropolishing retards hydrogen absorption and may severely limit hydrogen uptake. Absorption is also important in the hydride-forming alloys, and in fact, the results of our study indicate that there is no embrittlement of titanium alloys unless a hydride phase is formed either during the exposure or the test [6].

DISCUSSION OF RESULTS

Permeation

Permeability is a property of the material which in the ideal case is controlled only by the electronic and crystal structures. For metals with cubic symmetry, permeability is isotropic; therefore, permeability is unaffected by

texture that develops during processing. Metals or alloys with hexagonal symmetry, however, have a permeability that is different along the a- and c-axes. In such cases, texture in a fabricated part will have an influence on permeation rate. For example, the permeability of the ε-phase of cobalt which has a HCP lattice was derived from measurements on textured polycrystalline sheet; therefore, the data in FIG. 1 are an "average" of the permeabilities in the c- and a-directions. Data for the high-temperature α-phase of cobalt, which has a FCC lattice, is not subject to this restriction.

In all metals and alloys that have been investigated there is evidence of significant influence of both surface phenomena and internal defects and impurities on absorption and permeation of hydrogen, resulting in large deviations from ideal behavior [5,6,13,14,15,16,22]. Although these deviations have been observed for some time, current investigations of hydrogen transport are directed toward detailed elucidations. Existing mathematical models of surface processes or films and of internal trapping have been adapted to the permeation process [14]. Surface and internal processes may be distinguished under some experimental conditions. Several characteristic differences in permeation behavior due to internal trapping and a uniform surface film are shown in Table XII.

Surface Films

Oxides are probably the most common form of surface film on metals and alloys, since oxidation occurs readily and is seldom purposely controlled during the fabrication of large engineering structures. Besides, external conditions may often affect formation, continued growth, or reduction of oxide films. Hydrogen absorption or desorption is consequently retarded since oxides have a lower permeability than metals [10,21]. Moreover, during growth or reduction of an oxide film the oxide-metal interface acts as a source or sink for hydrogen vacancies and oxygen, both of which can trap diffusing hydrogen. The influence of an oxide film on hydrogen absorption and permeation will depend upon the stability of the oxide in the ambient environment, its crystal structure, film thickness, permeability relative to that of the metal, and its microstructural continuity and perfection. The effects of each of these oxide film characteristics have been observed in studies on Types 304 and 310 stainless steel [5], aluminum [25], and titanium alloys [6].

Trapping

Interaction between diffusing hydrogen and metal lattice defects and impurities can significantly retard hydrogen movement, resulting in an effective diffusivity that is lower than expected. A simple model proposed by McNabb and Foster [30] relates the overall diffusion to the number of trap sites and the probability of capture and release from the trap. Application of their model [15] demonstrated general conformity to experimental observations, although detailed interpretation of the experiments is not possible because of limitations in understanding the trapping process, its mathematical representation, and accuracy of experimental data. Sites that have been identified or are suspected as being traps include: dislocations in Type 304L stainless

steel, nickel, molybdenum, aluminum alloys, and iron [9,13]; interstitial or vacancy clusters in gold; oxygen in copper [20]; and grain or subgrain boundaries in nickel [16].

The hydrogen-dislocation interaction is especially important since it is intimately related to embrittlement. During plastic deformation of a metal, a dislocation may move inwardly from the external surface, dragging along absorbed hydrogen atoms at a faster rate than for diffusion alone. This increased mobility has been reported for Type 304L stainless steel tensile specimens tested in 69-MPa tritium. Concentrations of tritium along slip planes were also observed in autoradiographs. A free surface is also a dislocation sink; consequently hydrogen may be pulled out of the interior and rejected to the surrounding atmosphere as observed in tritium release from iron, Type 304L stainless steel, nickel, "Inconel" 718, and 5086 aluminum [9].

Failure Under Dynamic Conditions

Hydrogen embrittlement, as observed in tensile tests of materials, is characterized by increases with increasing hydrogen content, a maximum at an intermediate temperature, and a decrease with increasing strain rate [31]. These characteristics are seen, for example, in cathodically charged mild steel [31] and gas-phase-charged austenitic steels [7], nickel [32], and high strength steels [33]. Analogous characteristics are observed in hydrogen transport by dislocation [34]; therefore, dislocation transport of hydrogen is clearly significant in the embrittlement of metals that do not form hydrides. The concepts of binding of hydrogen t dislocations and of hydrogen movement with dislocations provided the basis for a phenomenological description of the embrittlement process that can explain the temperature-, strain rate-, and hydrogen-content dependence of hydrogen embrittlement as discussed earlier [9].

Transport of hydrogen into a region by dislocations during plastic deformation is given by the equations:

$$C_T \propto \rho m \, C_\perp \, \bar{V} \quad \text{and}$$

$$C_\perp = C_o \exp(-G_{B/RT}) \quad \text{where}$$

C_o is the nominal hydrogen concentration,

C_T is the amount of hydrogen transported,

$C_\perp$ is the hydrogen content at a dislocation core, ρm is the mobile dislocation density, $\bar{V}$ is the average dislocation velocity, and G_B is the binding energy which is negative for an attractive dislocation-hydrogen interaction. Several qualitative predictions follow from these equations:

- decreasing susceptibility with increasing temperature due to a decrease in the ratio $C_\perp/C_o$,
- decrease in C_T at low temperature due to decreased C_o or saturation of the dislocation, i.e., $C_\perp = 1$, or decreased hydrogen mobility,

- decreased embrittlement with increasing strain-rate, and

- temperature of maximum embrittlement increases with increasing strain-rate and increasing hydrogen content.

Further details of the mechanism by which dislocation transport of hydrogen reduces ductility in metals is currently being pursued.

Studies of susceptibility to hydrogen embrittlement have shown that loss of ductility is promoted by coplanar dislocation motion [35] and that susceptibility is greater for high strength alloys than for low strength alloys of similar structures [36]. Results of these studies provide simple criteria for alloy selection to minimize susceptibility to hydrogen embrittlement. Low hydrogen solubility is desirable, as indicated by the fact that neither copper nor aluminum is susceptible to dynamic embrittlement, and their hydrogen solubilities are much lower than those of alloys of iron and nickel, which are easily embrittled by hydrogen. Alloys that should be avoided in hydrogen service are those with low stacking-fault energies, large negative dislocation-hydrogen binding energies, and high-strengths; these are properties that promote embrittlement. Where these properties cannot be avoided, for example where high strength is needed, alloy design may assist in minimizing embrittlement. Fine dispersions of incoherent precipitates have been shown to be effective in eliminating deleterious hydrogen effects in nickel [37]. Prestraining in air prior to hydrogen exposure has reduced embrittlement in other alloys [38].

CONCLUSIONS

Investigations carried out during the past decade both at Savannah River Laboratory and other sites lead to general conclusions that:

- All structural alloys are susceptible in different degrees to hydrogen embrittlement, though conditions which maximize ductility losses vary among alloys. Aluminum alloys and copper alloys are relatively unaffected by hydrogen, whereas austenitic stainless steels are somewhat affected, and ferritic steels and nickel-base superalloys are strongly embrittled.

- Absorption and permeation of hydrogen in metals, as well as final distribution of absorbed hydrogen throughout a metal structure, cannot be predicted accurately by the usual thermodynamic and diffusion relations. Surface effects — particularly the properties and stability of oxide films under differing conditions, trapping of hydrogen by impurities and microstructural defects, and hydrogen transport by moving dislocations — all profoundly influence hydrogen motion and distribution, and therefore hydrogen embrittlement, since the quantity and distribution of absorbed hydrogen are directly related to the embrittlement mechanism.

- Performance of structural and equipment components exposed to hydrogen for long periods may be limited by material characteristics that increase susceptibility of metals to absorption and permeation of hydrogen. Therefore, optimum performance and service life of hydrogen-exposed materials demand careful analysis of service conditions, proper selection of materials, and effective quality control during all stages of processing and fabrication.

REFERENCES

[1] W. B. McPherson and C. E. Cataldo. "Recent Experience in High Pressure Gaseous Hydrogen Equipment Operated at Room Temperature." *Technical Report No. D814.1.* American Society for Metals, Metals Park, Ohio (1968).

[2] H. G. Nelson. "Hydrogen-Induced Slow Crack Growth." Presented at the *Int. Conf. on the Effect of Hydrogen on the Behavior of Materials,* Jackson, Wyoming, September 7-11, 1975.

[3] H. E. McCoy, Jr. *Effects of Hydrogen on the High-Temperature Flow and Fracture Characteristics of Metals.* USAEC Report ORNL-3600 (June 1964).

[4] H. L. Marcus. "Crack Growth and Fracture in Hydrogen Gas." Presented at the *Int. Conf. on the Effect of Hydrogen on the Behavior of Materials,* Jackson, Wyoming, September 7-11, 1975.

[5] M. R. Louthan and R. G. Derrick. "Hydrogen Transport in Austenitic Stainless Steel." *Corrosion Science 15* (9), 565 (1975).

[6] G. R. Caskey, Jr. "The Influence of a Surface Oxide Film on Hydriding of Titanium." p 465 in *Hydrogen in Metals,* ASM, Metals Park, Ohio (1974).

[7] M. R. Louthan, Jr. "Effects of Hydrogen on the Mechanical Properties of Low Carbon and Austenitic Steels." p 53 in *Hydrogen in Metals,* ASM, Metals Park, Ohio (1974).

[8] M. R. Louthan and A. H. Dexter. "Hydrogen Embrittlement of Aluminum." *Met. Trans. A 6A,* 1655 (1975).

[9] M. R. Louthan, G. R. Caskey, J. A. Donovan, and D. E. Rawl. "Hydrogen Embrittlement of Metals." *Mat. Sci. Eng. 10,* 357 (1972).

[10] G. R. Caskey, Jr. "Diffusion of Tritium in Rutile." *Mat. Sci. Eng. 14,* 109 (1974).

[11] G. R. Caskey, R. G. Derrick and M. R. Louthan. "Hydrogen Diffusion in Cobalt." *Scripta Met. 8,* 481 (1974).

[12] M. R. Louthan, J. A. Donovan, and G. R. Caskey. "Isotope Effects on Hydrogen Transport in Nickel." *Scripta Met. 8,* 643 (1974).

[13] G. R. Caskey, M. R. Louthan, and R. G. Derrick. "Hydrogen Transport in Molybdenum." *J. Nucl. Mater. 55,* 279 (1975).

[14] G. R. Caskey and W. L. Pillinger. "Effect of Trapping on Hydrogen Permeation." *Met. Trans. A 6A,* 467 (1975).

[15] M. R. Louthan, J. A. Donovan, and G. R. Caskey, Jr. "Tritium Absorption in Type 304L Stainless Steel." *Nucl. Technol. 26,* 192 (1975).

[16] M. R. Louthan, J. A. Donovan, and G. R. Caskey. "Hydrogen Diffusion and Trapping in Nickel." *Acta Met. 23,* 745 (1975).

[17] M. R. Louthan, G. R. Caskey, and J. A. Donovan. "Metallographic Studies of Hydrogen-Embrittled Nickel." *Microstructural Science 3 (B),* 823. American Elsevier Pub. Co. Inc., New York (1975).

[18] M. R. Louthan. "The Effect of Hydrogen on Metals." *NACE Corrosion Short Course,* St. Louis, Sept. 9-13, 1974.

[19] M. R. Louthan, D. E. Rawl, J. A. Donovan, and W. G. Holmes. "Hydrogen Embrittlement of Austenitic Stainless Steel." To be published in *Nucl. Technol.*

[20] G. R. Caskey, A. H. Dexter, M. L. Holzworth, M. R. Louthan, and R. G. Derrick. "Hydrogen Transport in Copper." Submitted to *Corrosion.*

[21] G. R. Caskey. "Surface Effects on Tritium Diffusion in Materials in a Radiation Environment." *Symposium on Radiation Effects on Solid Surfaces,* American Chemical Society, August 25-26, 1975.

[22] M. R. Louthan, R. G. Derrick, J. A. Donovan, and G. R. Caskey. "Hydrogen Transport in Iron and Steel." Presented at *International Conference on Effect of Hydrogen on Behavior of Materials,* September 7-11, 1975.

[23] M. R. Louthan and R. G. Derrick. "Permeability of Nickel to Hydrogen Isotopes." To be published in *Scripta Met.*

[24] M. R. Louthan, G. R. Caskey, D. E. Rawl, and C. W. Krapp. "Tritium Effects in Austenitic Steel." *Conf. on Radiation Effects and Tritium Technology for Fusion Reactors,* Gatlinburg, Tennessee, October 1-3, 1975.

[25] M. R. Louthan, G. R. Caskey, and A. H. Dexter. "Hydrogen Effects in Aluminum Alloys." *Conf. on Radiation Effects and Tritium Technology for Fusion Reactors,* Gatlinburg, Tennessee, October 1-3, 1975.

[26] R. P. Jewett et al. *Hydrogen Environment Embrittlement of Metals,* NASA CR-2163, Rocketdyne, Canoga Park, California (March 1973).

[27] J. P. Fidelle et al. "Disc Pressure Testing of Environmental Hydrogen Embrittlement." p 221 in STP 543, *Hydrogen Embrittlement Testing,* American Society for Testing Materials, Philadelphia, PA (1974).

[28] M. O. Speidel. "Hydrogen Embrittlement of Aluminum Alloys." p 249 in *Hydrogen in Metals*, ASM, Metals Park, Ohio (1974).

[29] R. M. Vennett and G. S. Ansell. "A Study of Gaseous Hydrogen Damage in Certain FCC Metals," *Trans. ASM 62*, 1007 (1969).

[30] A. McNabb and P. K. Foster. "A New Analysis of the Diffusion of Hydrogen in Iron and Ferritic Steels," *Trans. AIME 227*, 618, 1963.

[31] T. Toh and W. M. Baldwin, Jr. *Stress Corrosion Cracking and Embrittlement*, W. D. Robertson ed, p 176, J. Wiley and Sons, New York (1969).

[32] G. C. Smith. "Effect of Hydrogen on Nickel." p 485 in *Hydrogen in Metals*, ASM, Metals Park, Ohio (1974).

[33] W. Beck, E. J. Jankowsky and P. Fischer. *Hydrogen Stress Cracking of High Strength Steels*. NADC-MA-7140, Naval Air Development Center, Warminster, PA (December 1971).

[34] J. A. Donovan. "Accelerated Evolution of Hydrogen During Plastic Deformation." Presented at the *Fifth Annual Spring Meeting, Institute of Metals Division, AIME*, Philadelphia, Pennsylvania, May 29-June 1, 1973.

[35] P. Cotterill. *Progress in Materials Science, Vol. 9*, p. 20. Pergamon Press, Oxford, London, New York, and Paris (1961).

[36] D. P. Williams and H. G. Nelson. "Discussion of Evaluation of Hydrogen Embrittlement Mechanisms." *Met. Trans. 2*, 1987 (1971).

[37] A. W. Thompson and B. A. Wilcox. "Deformation and Fracture of Dispersion-Strengthened Nickel Charged With Hydrogen." *Scripta Met. 6*, 689 (1972).

[38] D. D. Perlmutter and B. F. Dodge. "Effects of Hydrogen on Properties of Metals." *Ind. Eng. Chem. 48*, 885 (1956).

TABLE I

Hydrogen Effects on Copper Alloys

Alloy	*Test Environment*	*Strength, MPa*		*Ductility*	
		Yield	*Ultimate*	*Red. Area, %*	*Elong., %*
Oxygen-free	0.1-MPa Air	96.5	234	71	44
	69-MPa H_2	96.5	228	71	45
Boron Deoxidized	0.1-MPa Air	96.5	234	92	40
	0.1-MPa Air[a]	55.2	200	92	49
	69-MPa H_2	68.9	214	94	46
	69-MPa H_2[a]	41.4	200	96	51
70-30 Brass	0.1-MPa Air	124	365	70	59
	0.1-MPa Air[a]	89.6	372	80	59
	69-MPa H_2	103	345	84	58
	69-MPa H_2[a]	96.6	363	83	57
	69-MPa He[b]	572	607	69	8
	69-MPa H_2[b]	579	607	70	8
Aluminum Bronze	0.1-MPa Air	224	600	67	48
	69-MPa H_2	212	576	71	49
	69-MPa H_2[f]	220	631	69	51
"Berylco-25"	69-MPa He[c]	179	434	76	52
	69-MPa H_2	179	441	69	51
	69-MPa He[d]	283	531	52	29
	69-MPa H_2	296	586	54	30
	69-MPa He[e]	1069	1220	9	5
	69-MPa H_2	1076	1186	7	4

a. Prior exposure 300 MPa H_2 at 473°K for 56 days.

b. 50% cold worked.

c. Annealed.

d. One-fourth hard.

e. One-half hard.

f. Prior exposure 10 atm. H_2 at 580°K for 48 hours.

TABLE II

Hydrogen Effects on Nickel Alloys

Alloy	Test Environment	Strength, MPa		Ductility	
		Yield	Ultimate	Red. Area, %	Elong., %
Nickel	69-MPa He	186	427	79	57
	69-MPa H_2	172	434	54	47
Nickel (HERF)	69-MPa He	571	600	85	23
	69-MPa He	600	620	66	13
Nickel TD	69-MPa He	214	338	87	19
	69-MPa H_2	214	352	72	20
"Inconel" 718[a]	69-MPa He	1041	1282	40	25
	69-MPa H_2	1069	1262	11	9
"Inconel"[b]	0.1-MPa Air	372	731	66	37
	0.1-MPa Air[c]	372	703	43	34
	69-MPa He	338	703	69	39
	69-MPa H_2	345	689	27	25
"Inconel" 700[d]	0.1-MPa Air	1048	1406	45	21
	69-MPa He	1034	1344	44	22
	69-MPa H_2	1027	1220	14	10
	69-MPa H_2	938	1034	7	8
"Hastelloy" X[e]	0.1-MPa Air	324	689	69	56
	0.1-MPa Air[c]	324	696	41	49
	69-MPa He	283	689	68	59
	69-MPa H_2	289	655	58	55
	69-MPa H_2[c]	338	538	36	29
Waspaloy	0.1-MPa Air	517	841	66	50
	0.1-MPa Air[c]	524	765	28	29
	69-MPa He	503	848	65	50
	69-MPa H_2	462	738	28	26
"Rene 41"[f]	0.1-MPa Air	1069	1317	41	23
	0.1-MPa Air[c]	1117	1179	10	4
	69-MPa He	1089	1365	39	23
	69-MPa H_2	1082	1255	12	12
Ni-2% Be	0.1-MPa Air	1270	1612	9	5.0
	69-MPa H_2	986	988	2	0.5

a. Trademark of International Nickel for 19% Cr, 5% Nb, 3% Mo, 0.9% Ti, 0.5% Al, 18.5% Fe, balance nickel.

b. Trademark of International Nickel for 15% Cr, 1.6% Si, 2% (Nb and Ti) 9% Fe, balance nickel.

c. Prior exposure 69-MPa H_2 at 428°K for 1000 hr.

d. Trademark of International Nickel for 15% Cr, 30% Co, 3% Mo, 12% Ti, 3% Al, balance nickel.

e. Trademark of Cabot Corp. for 22% Cr, 1.5% Co, 9% Mo, 0.5% W, 18% Fe, balance nickel.

f. Trademark of General Electric for 19% Cr, 11% Co, 10% Mo, 3% Ti, 1.5% Al, balance nickel.

TABLE III

Hydrogen Effects on Titanium and Miscellaneous Alloys

Alloy	*Test Environment*	*Strength, MPa*		*Ductility*	
		Yield	*Ultimate*	*Red. Area, %*	*Elong., %*
Titanium	0.1-MPa Air	600	696	49	22
	69-MPa He	517	641	51	21
	69-MPa H_2	531	655	50	21
Ti-5Al-2½Sn	0.1-MPa Air	876	917	42	17
	69-MPa He	855	910	43	19
	69-MPa H_2	862	924	44	17
Ti-6Al-4V	0.1-MPa Air	979	1041	44	12
	69-MPa He	951	1020	45	13
	69-MPa H_2	951	1013	43	14
		Miscellaneous			
Tungsten	0.1-MPa Air	-	689	-	-
	0.1-MPa Air[a]	-	703	-	-
Molybdenum	0.1-MPa Air	-	724	-	-
	0.1-MPa Air[a]	-	717	-	-
W-25% RH	0.1-MPa Air	-	1227	-	-
	0.1-MPa Air[a]	-	1255	-	-
Mo-50% Rh	0.1-MPa Air	--	1930	-	-
	0.1-MPa Air[a]	-	1924	-	-
"Kovar"	0.1-MPa Air	400	558	-	23
	69-MPa H_2[b]	400	538	-	22
	69-MPa H_2[c]	400	552	-	24

a. Prior exposure to 69-MPa H_2 for 30 days at 428°K and 10 days at 300°K.

b. Prior exposure to H_2 at 344°K for 2 years.

c. Prior exposure to H_2 at 428°K for 2 years.

TABLE IV

Tensile Properties of Austenitic Steels in 69-MPa Hydrogen and Helium[a]

Alloy	Test Environment	Strength, MN/m^2		Ductility	
		Yield	Ultimate	Elong. %	Red. Area %
216	He	586	786	45	70
	H_2	593	779	44	69
310	He	179	483	67	82
	H_2	186	486	66	79
21-6-9	He	352	689	58	78
	H_2	358	696	59	77
22-13-5	He	406	683	47	74
	H_2	406	683	45	73
X18-3	He	530	792	50	74
	H_2	524	786	46	73
347	He	206	572	60	80
	H_2	200	510	38	37
316	He	214	496	68	78
	H_2	214	524	72	77
309S	He	276	579	60	71
	H_2	262	586	63	74
304N	He	641	848	43	74
	H_2	641	841	36	54
"Tenelon"[b]	He	496	876	65	68
	H_2	496	903	55	47
304L	He	186	565	74	81
	H_2	206	503	48	33
A-286	He	724	1117	26	47
	H_2	710	1131	34	49
CG-27	He	806	1165	29	26
	H_2	855	1117	10	12
18-13-2[b]	Air	730	1007	51	58
	H_2	662	924	33	27

a. Data averages of at least two specimens.

b. Trademark of U.S. Steel for 18% Cr, 15% Mn, 0.5% N balance iron.

c. HERF condition.

TABLE V

Tensile Properties of Austenitic Steels Thermally Charged by Exposure to High Pressure Hydrogen

	Charging Conditions				*Strength, MN/m^2*		*Ductility*	
Alloy	*Pressure, MPa*	*Temp., °K*	*Time, hr.*	*Test Environment*	*Yield*	*Ultimate*	*Elong., %*	*Red. Area, %*
216	69	425	1000	69-MPa H_2	565	765	45	64
	69	425	1000	Air	634	792	36	65
CG-27	69	425	720	69-MPa H_2	855	1020	4	3
21-6-9	69	475	500	Air	455	780	50	41
304N	69	425	1000	69-MPa H_2	551	792	37	46
	69	425	1000	Air	737	834	31	65
"Tenelon"	69	425	1000	69-MPa H_2	468	758	24	23
	69	425	1000	Air	551	841	36	41
A-286	69	450	4800	Air	744	1034	12	14
304L	69	450	4800	Air	220	530	33	31
310	69	425	1000	69-MPa H_2	179	441	70	80
	69	425	1000	Air	200	496	63	76

TABLE VI

Tensile Properties of Austenitic Stainless Steels Tested in Air After Prolonged Hydrogen Exposure

Alloy	*Exposure*	*Strength, MN/m²*		*Ductility*		*Dislocation Substructure*
		Yield	*Ultimate*	*Red. Area, %*	*Elong., %*	
304L						
Normal	None	213	600	77	73	Coplanar
	10^4-psi H_2	220	530	32	33	
HERF[a]	None	551	682	76	35	Tangles
	10^4-psi H_2	579	717	68	41	
310	None	214	534	79	61	Mixed
(Normal)	10^4-psi H_2	200	496	76	63	
"Tenelon"	None	572	930	65	56	Coplanar
(Normal	10^4-psi H_2	551	841	36	41	
21-6-9						
Normal	None	434	744	56	56	Coplanar
	10^4-psi H_2	431	724	28	30	
HERF	None	607	792	74	32	Tangles
	4000-psi H_2	655	820	59	31	

---

a. High energy rate forming.

TABLE VII

Tensile Properties of HERF Austenitic Stainless Steels

Alloy	*Test Environment*	*Strength, MN/m²*		*Ductility*	
		Yield	*Ultimate*	*Elong., %*	*Red. Area, %*
310	69-MPa He	468	606	21	71
	69-MPa H_2	462	620	24	70
21-6-9	69-MPa He	572	779	34	75
	69-MPa H_2	572	792	30	73
304L	69-MPa He	489	661	43	77
	69-MPa H_2	489	668	41	69
A-286	Air	875	1062	24	29
	69-MPa H_2	834	1110	27	32
18-13-2	Air	730	1007	51	58
	69-MPa H_2	661	923	33	27
CG-27	69-MPa He	1069	1385	12	12
	69-MPa H_2	1034	1138	1	3

TABLE VIII

Effects of Deuterium Exposure on Annealed 3003 Aluminum

Exposure	*Test Temperature, °K*	*Strength, MPa*		*Elong., %*
		Yield	*Ultimate*	
None	383	30.3	81.4	35
	343	29.6	91.7	32
	303	42.7	111.7	20
	263	39.3	110.3	32
	223	42.7	111.7	35
D_2 Gas[a]	383	34.5	77.2	33
	343	39.3	86.2	31
	303	42.7	97.9	23
	263	32.4	100.7	31
	223	48.9	106.2	27
LiD + D_2 gas[a]	383	42.1	83.4	32
	343	38.6	92.4	31
	303	40.0	95.1	24
	263	38.6	99.3	26
	223	47.6	107.6	27

a. 69-MPa pressure deuterium gas for 28 hours.

TABLE IX

Hydrogen Effects on Aluminum Alloys

Alloy	*Test Environment*	*Strength, MPa*		*Ductility*	
		Yield	*Ultimate*	*Red. Area, %*	*Elong., %*
2011	0.1-MPa	269	338	48	17
	69-MPa He	227	296	57	18
	69-MPa H_2	220	296	58	17
2024	0.1-MPa Air	358	489	33	15
	69-MPa He	324	441	36	19
	69-MPa H_2	310	427	35	18
5086	0.1-MPa Air	193	303	49	18
	69-MPa He	151	248	55	20
	69-MPa H_2	138	248	57	21
6061	0.1-MPa Air	179	234	75	14
	69-MPa He	131	179	82	15
	69-MPa H_2	138	186	82	14
6063	0.1-MPa Air	214	241	62	13
	69-MPa He	158	193	83	15
	69-MPa H_2	158	200	84	15
7039	0.1-MPa Air	152	179	80	14
	69-MPa He	124	138	85	14
	69-MPa H_2	117	138	86	14

TABLE X

Effect of Prolonged Hydrogen Exposure
on the Tensile Properties of 7039 Aluminum

Condition	σ_y, *MPa*	σ_{ult}, *MPa*	*Ductility*	
			Red. Area, %	*Elong., %*
Unexposed	303	379	44	13
Exposed[a]	310	372	45	14

---

a. Exposed 524 days to 69-MPa H_2 at 343°K; data averages of at least three samples.

TABLE XI

Effects of Tritium Exposure on the Mechanical
Properties of 1100 Aluminum at 300°K

Exposure	σ_y, *MPa*	σ_{ult}, *MPa*	*% Elong. in 2.54 cm*
None	34	90	32
	49	90	33
69-MPa for	34	96	36
38 days	41	96	39
at 343°K	34	96	34
69-MPa	41	90	29
for 510 days	41	90	33
at 343°K	41	90	30

TABLE XII

Effects of Trapping and Surface Films on Permeation

	Reversible Trapping	*Irreversible Trapping*	*Continuous Film*
Steady-State Permeation Rate (P_∞)	$P_\infty = P_\infty$ (ideal)	$P_\infty = P_\infty$ (ideal)	$P_\infty < P_\infty$ (ideal)
Apparent Diffusivity (D*)	$D^* < D_L$	$D^* < D_L$ [a]	$D^* < D_L$
Instantaneous Permeation Rate (P_t)	$P_t < P_t$ (ideal)	$P_t < P_t$ (ideal)	$P_t < P_t$ (ideal)
Instantaneous Evolution Rate (E_t)	$E_t > E_t$ (ideal)	$E_t = E_t$ (ideal)	$E_t < E_t$ (ideal)

---

a. D_L = true lattice diffusivity.

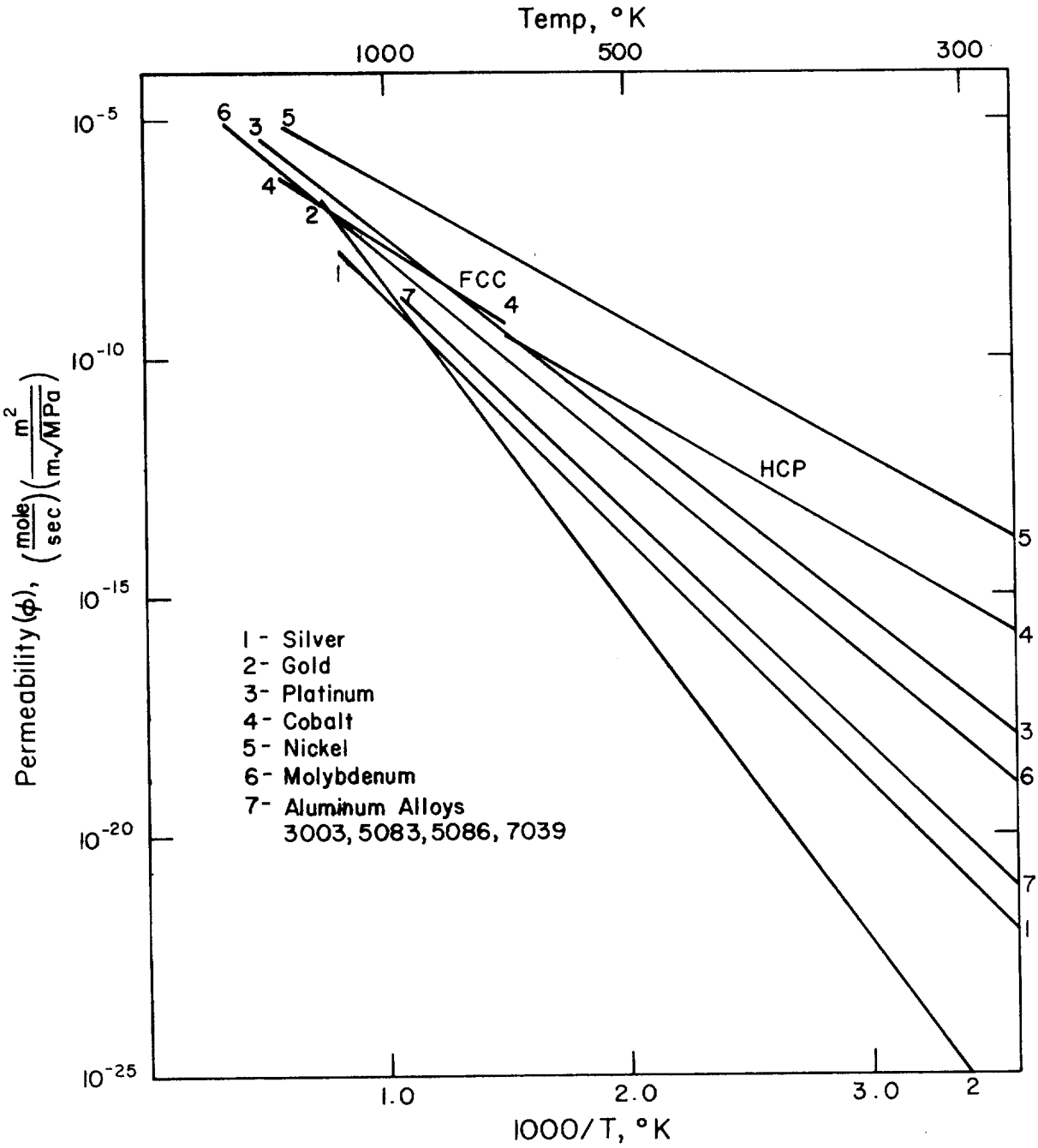

FIG. 1. Hydrogen Permeability in Aluminum Alloys and Other Metals

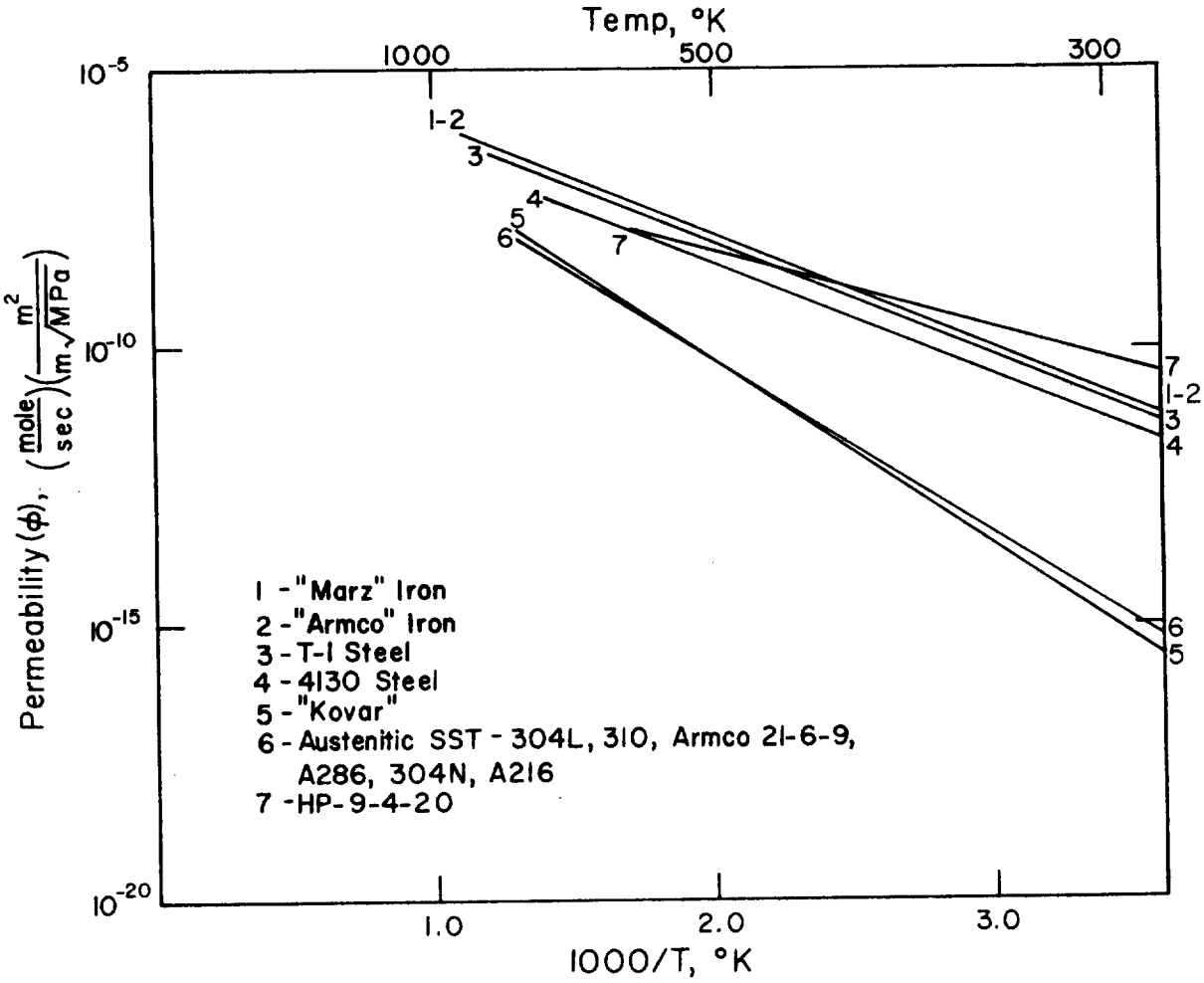

FIG. 2. Hydrogen Permeability of Ferritic and Austenitic Steels

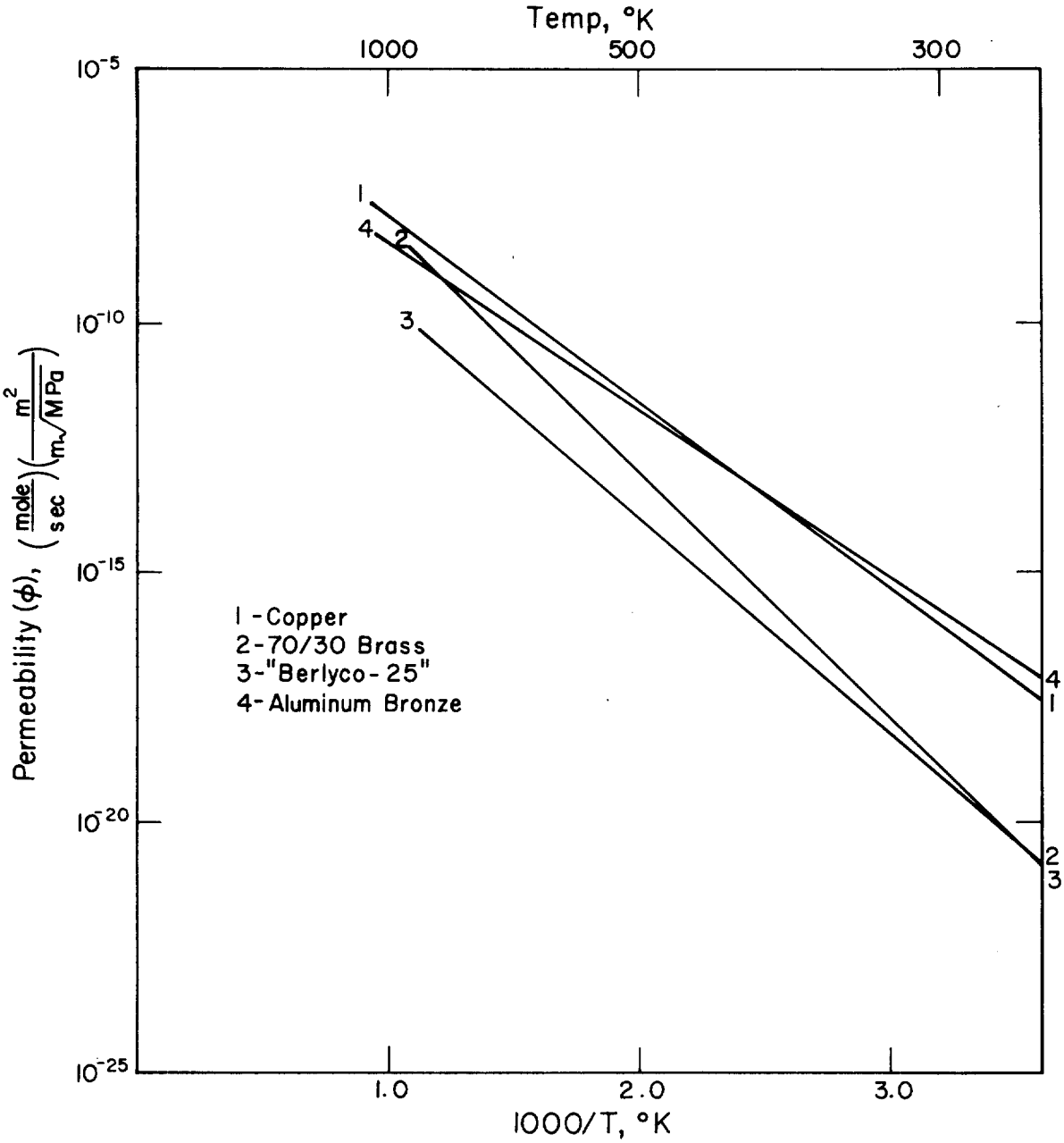

FIG. 3. Hydrogen Permeability of Copper Alloys

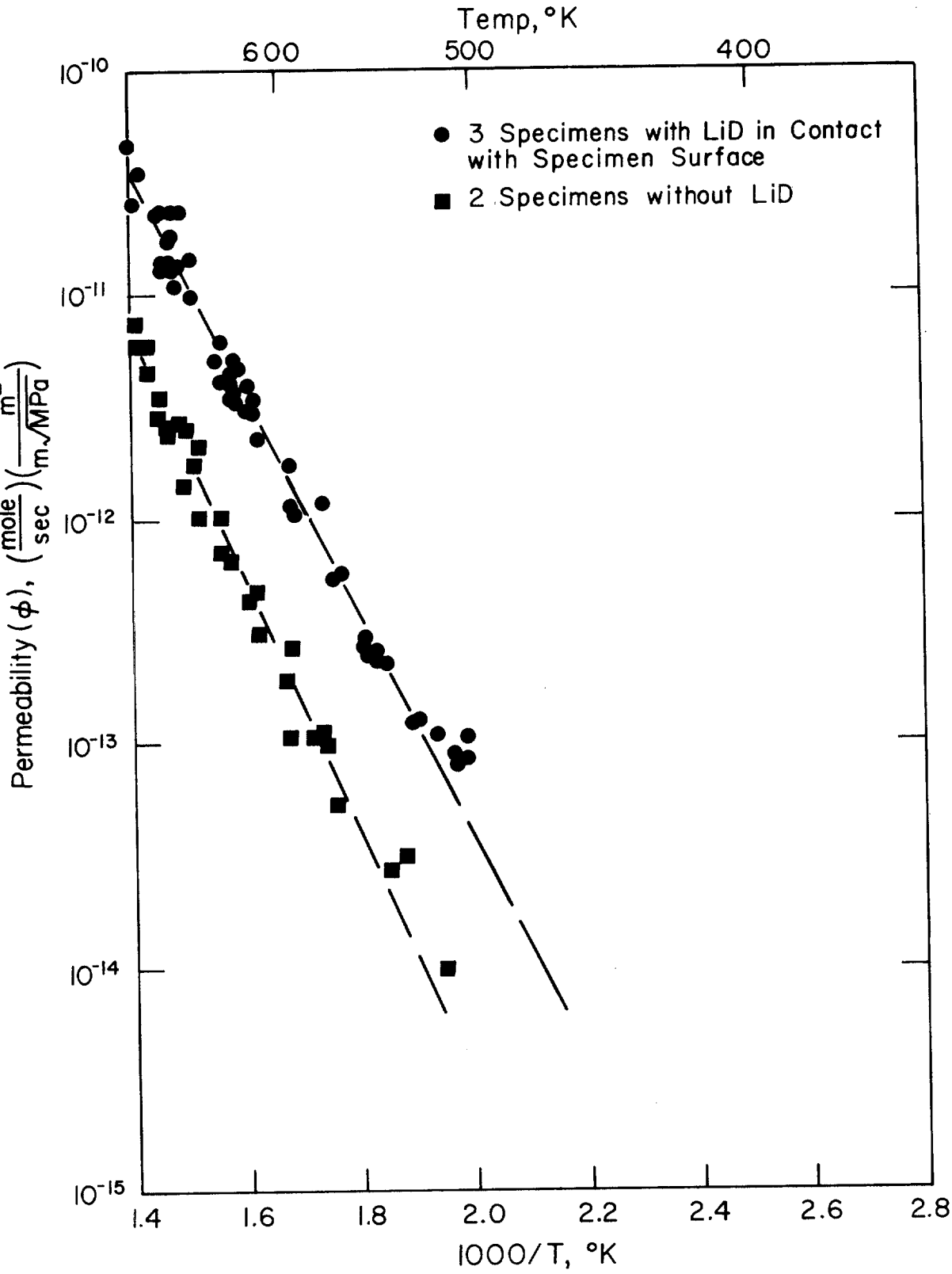

FIG. 4. Effect of LiD on the Permeability of Deuterium Through 3003 Aluminum

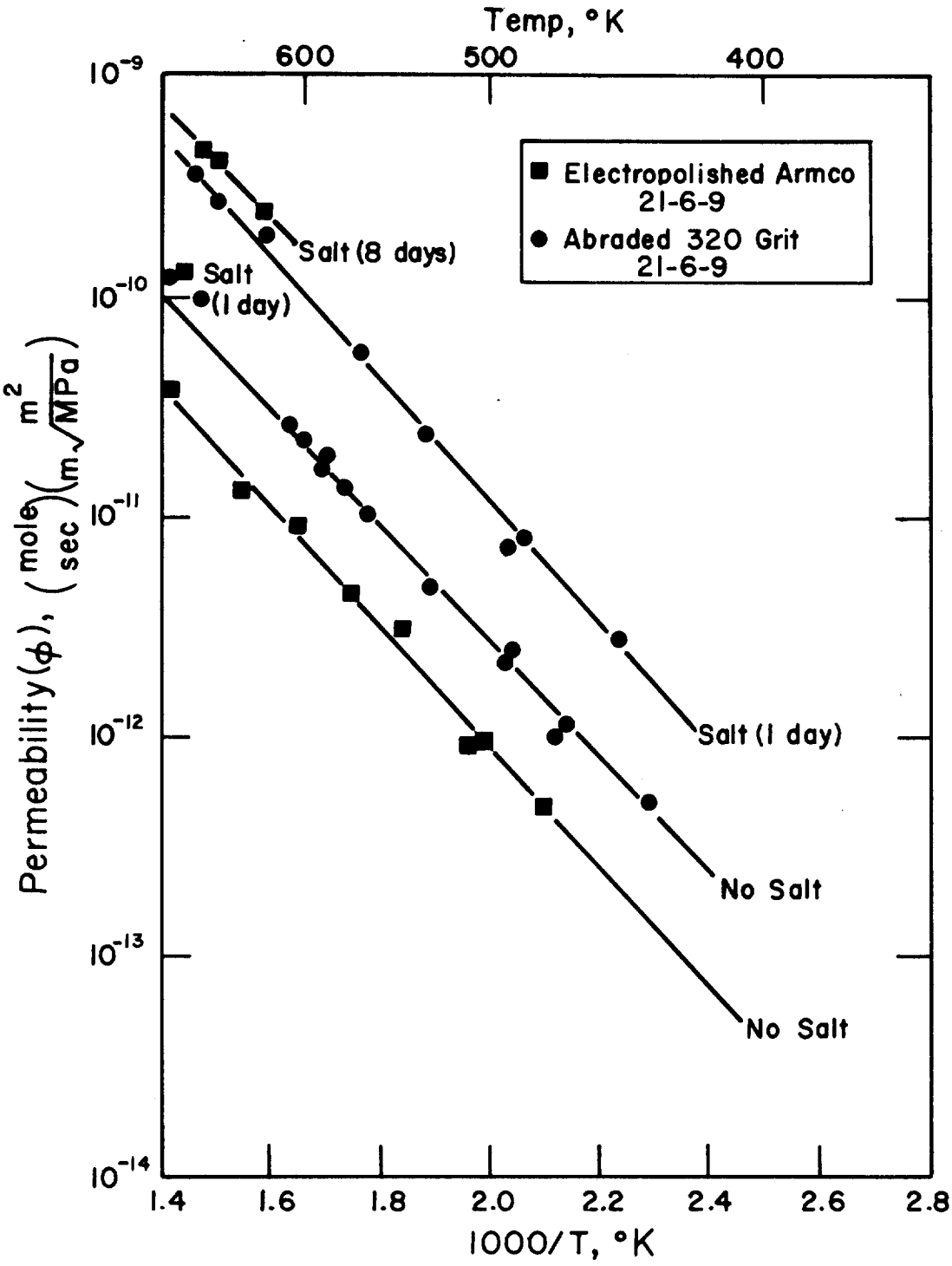

FIG. 5. Effect of LiD in Permeation Cell on Apparent Steady-State Permeability (All Specimens First Studied with LiD Present)